Supporting Information

Atomic Precision Engineering of Heterometallic Hexanuclear Al/M MOFs for Supercapacitor Applications

Bo Yan[a], Wenjuan Ji[a,*], Shucong Fan[b], Weiwei Pei[a], Guifang Liu[a], Bingqiang Wang[a], Quanguo Zhai[b,*], Yunlong Fu[a,*]

[a]Key Laboratory of Magnetic Molecules and Magnetic Information Materials Ministry of Education & School of Chemistry and Chemical Engineering of Shanxi Normal University, Taiyuan, Shanxi, 030032, PR China

[b]Key Laboratory of Applied Surface and Colloid Chemistry (MOE), School of Chemistry & Chemical Engineering, Shaanxi Normal University, Xi'an, Shaanxi, 710062, China.

*Corresponding author.

E-mail address: *jiwj@sxnu.edu.cn; zhaiqg@snnu.edu.cn;yunlongfu@sxnu.edu.cn.*

Contents

1. General materials and methods

All experimental materials and reagents were procured from commercial suppliers without further purification. Infrared spectra were recorded using PerkinElmer Fourier transform infrared (FTIR) spectroscopy instruments, with dried KBr powder serving as a matrix. The FT-IR spectrum was measured in the range of 4000-400 cm^{-1}. Powder X-ray diffraction (PXRD) data was collected on a Ultima Model IV-185 powder diffractometer with Cu-Kα radiation (40 kV, 40 mA). Thermal gravimetric analysis (TGA) was carried out on a Q600 thermal analyzer and heated from room temperature to 800 °C at a heating rate of 10 °C min^{-1} under a nitrogen atmosphere. The morphology of the synthesized material was characterized by field emission scanning electron microscope (SEM; JSM-7500F, Japan) and TEM (JEDL-JEM F200). ICP-MS analysis was conducted using the NexIONTM 300X.

Table S1. Crystal data and structure refinement for SXNU-20-Al/Mn, SXNU-20-Al/Ni

Compounds	SXNU-20-Al/Ni
Empirical formula	$C_{102}H_{108}Al_4Ni_2N_{11}O_{41}$
Formula weight	2369.33
Crystal system	cubic
Space group	*I*23
a (Å)	27.3691(7)
b (Å)	27.3691(7)
c (Å)	27.3691(7)
α (°)	90.00
β (°)	90.00
γ (°)	90.00
Volume/Å^3	20501.3(16)
Z	6
ρ_{calc} g / cm^3	1.151
μ / mm^{-1}	0.376
F (000)	7398.0
Crystal size/mm^3	0.30 × 0.27 × 0.22
2θ	4.706 - 52.736°
Reflections collected	104432
Independent reflections	7006
Data/restraints/parameters	7006/400/293
Goodness-of-fit on F^2	1.039
Final *R* indexes [$I \geq 2\sigma$ (I)]	R_1 = 0.0920, wR_2 = 0.2448
R indexes [all data]	R_1 = 0.1628, wR_2 = 0.3020
Largest diff. peak/hole/e Å^{-3}	1.29/-0.53

Table S2. Selected bonded lengths (Å) and angles (°) for SXNU-20-Al/Ni

Ni1-N1	2.094(7)	Al1-O2	1.947(11)
Ni1-O1	2.032(9)	Al1-O4	2.229(9)
Ni1-O1[a]	2.032(9)	Al1-O6	1.836(5)
Ni1-O3	2.063(8)	Al1-O7	2.123(10)
Ni1-O3[a]	2.063(8)	Ni1-O6	2.047(7)
N1-Ni1-O1[a]	90.5(9)	O1-Ni1-N1	87.1(9)
N1-Ni1-O1	87.1(9)	O1-Ni1-O3	89.2(2)
O2-Al1-O4	101.2(5)	O2-Al1-Al1[a]	118.1(4)
O6-Al1-O2	91.3(4)	O6–Al1–O4	79.6(3)
A11[a]–O6–Ni1	126.86(18)	Al1–O6–Ni1	126.86(18)
A11[a]–O6–Al1	106.3(4)	Al1–O7–Al1[b]	98.2(6)

Symmetry codes: (a) 1-X, -Y, +Z; (b) +X, -Y, -Z; (c) 1-Y, +Z, 1-X; (d) 1-Z, -X, -Y, (e) 1+Y, -Z, 1-X, (f) 1-Z, 1+X, -Y, (g) 1-Z, 1-X, Y, (h) 1/2-Y, -1/2+Z, 1/2-X.

Table S3. ICP-MS of SXNU-20-Al/M (M = Mn, Co, Ni)

materials	percentage of mass (wt%)	
	Al	M
SXNU-20-Al/Mn	8.1	7.6
SXNU-20-Al/Co	9.9	8.7
SXNU-20-Al/Ni	8.2	8.4

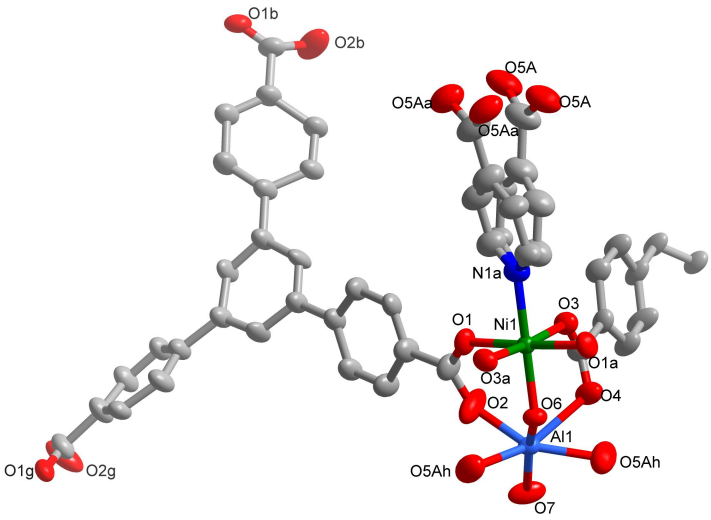

Fig. S1. Coordination environment diagram for SXNU-20-Al/Ni

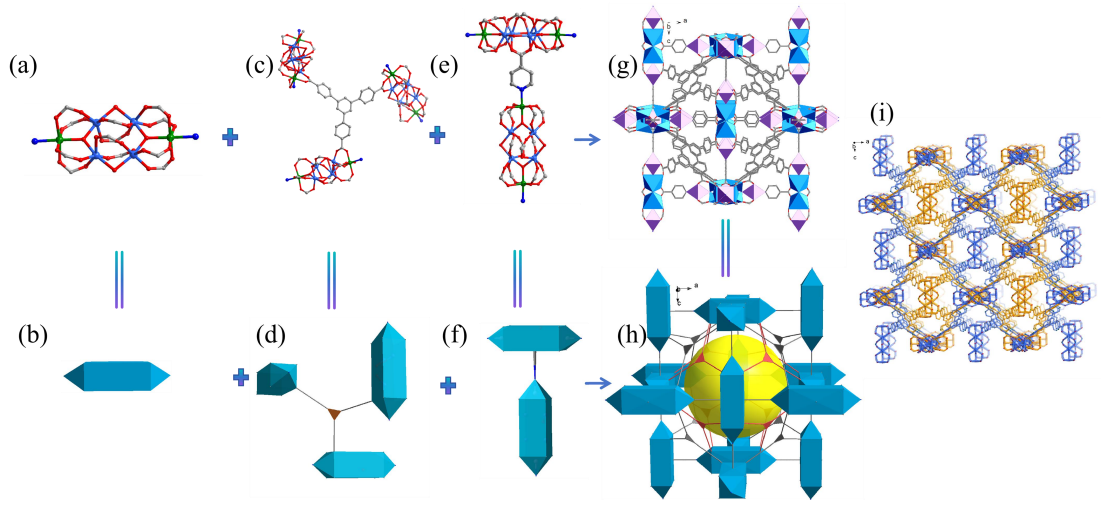

Fig. S2. Two interpenetrated networks connected by INA ligand form the non-interpenetrated framework SXNU-20-Al/Ni. (a, b) hexanuclear cluster and its simplified 12-connected node, (c, d) BTB^{3-} and INA ligands and their simplification, (e, f) the structure of the cage and (g, h) its topology network, (i) two interpenetrated networks.

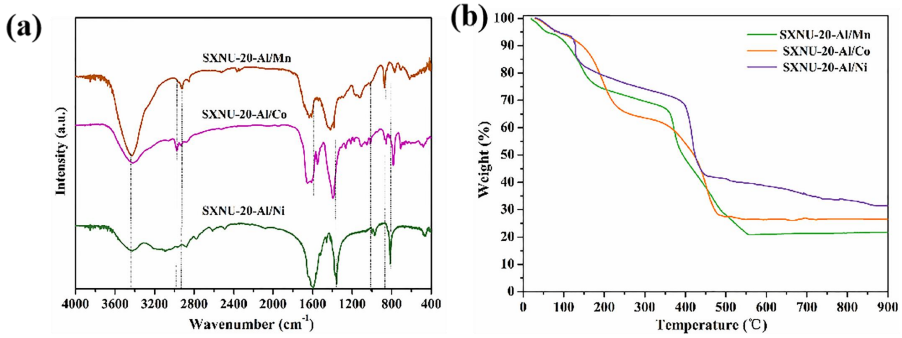

Fig. S3. (a) FT-IR spectra of compounds SXNU-20-Al/M (M = Mn, Co, and Ni); (b) thermogravimetric curves of compounds SXNU-20-Al/M (M = Mn, Co, and Ni).

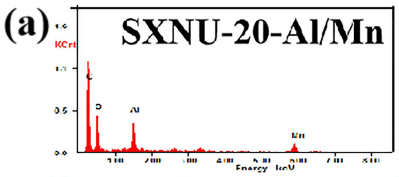

Element	Wt %	At %
C K	61.04	70.99
O K	28.76	25.11
AlK	04.98	02.58
MnK	05.22	01.33

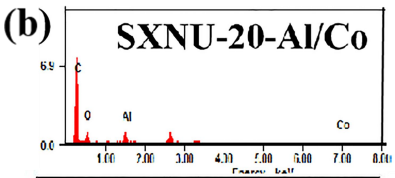

Element	Wt %	At %
C K	76.89	83.34
O K	18.43	15.00
AlK	02.41	01.16
CoK	02.27	00.50

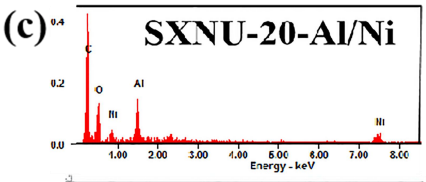

Element	Wt %	At %
C K	64.95	76.56
O K	20.99	18.57
AlK	05.21	02.73
NiK	08.85	02.13

Fig. S4. EDS of SXNU-20-Al/M (M = Mn, Co, Ni)

$$C_{sp}=\frac{I\triangle t}{m\triangle V} \quad \text{(S1)}$$

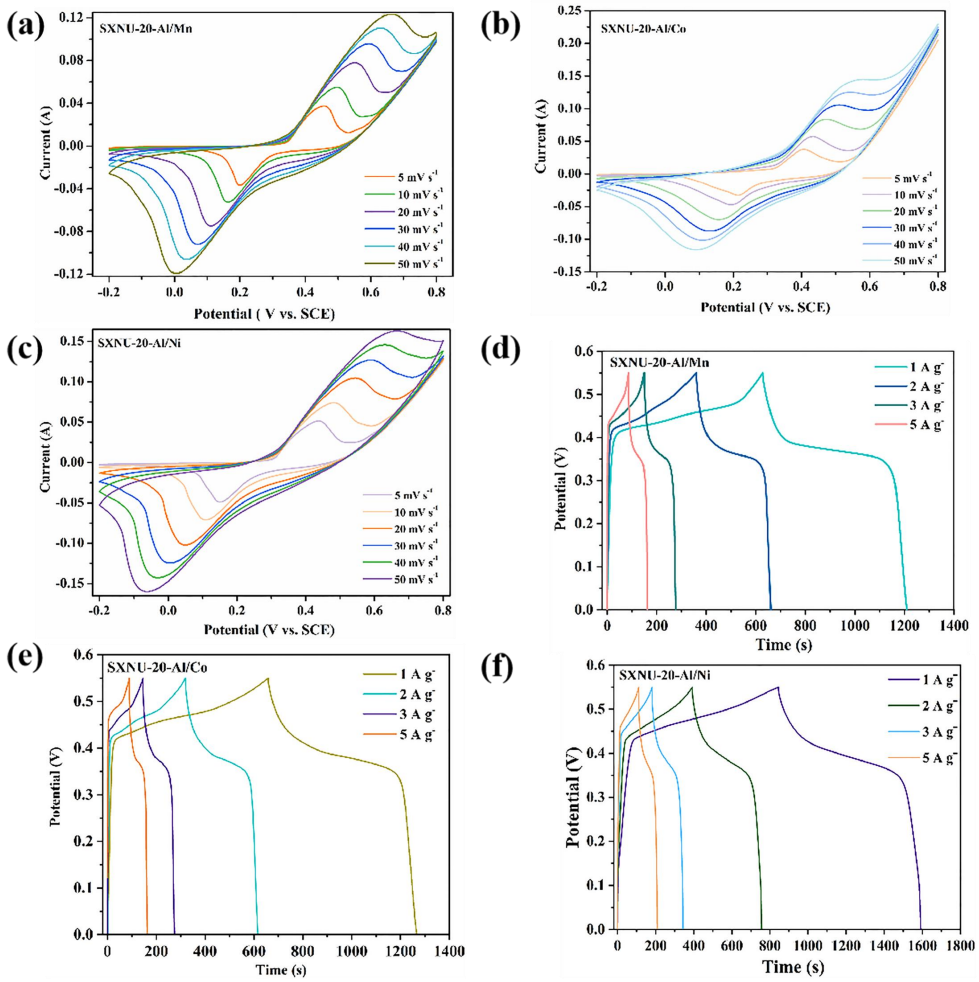

Fig. S5. CV curves for SXNU-20-Al/M (M = Mn, Co, Ni) MOF electrodes materials, (a-c) at varying scan rates of 5 to 50 mV s^{-1}; (d-f) Galvanostatic charge-discharge curves for SXNU-20 at various current densities from 1 to 5 A g^{-1}.

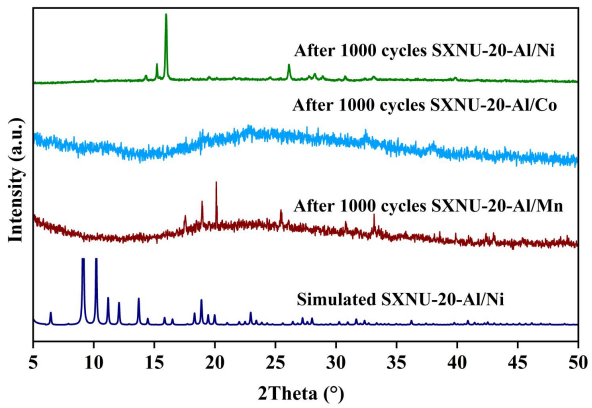

Fig. S6. The PXRD patterns after 1000 cycles.

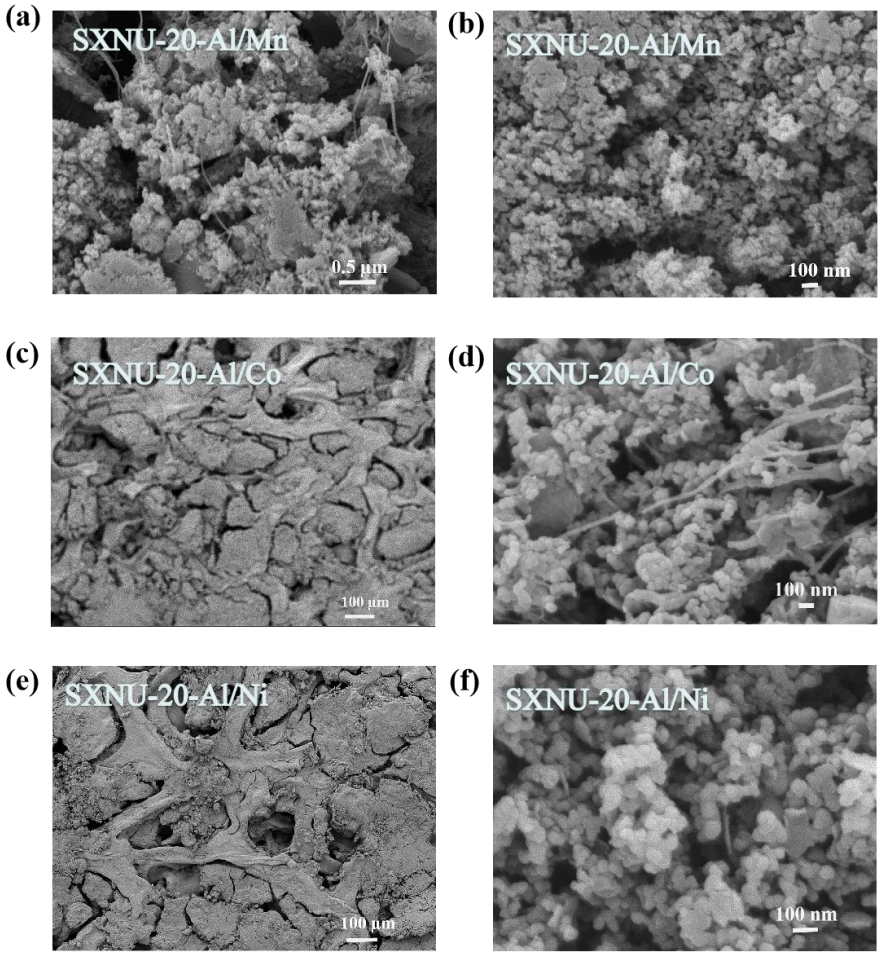

Fig. S7. (a-f) After the cycling scanning electron microscopy (SEM) of the SXNU-20-Al/M coating on the foam Ni plate.

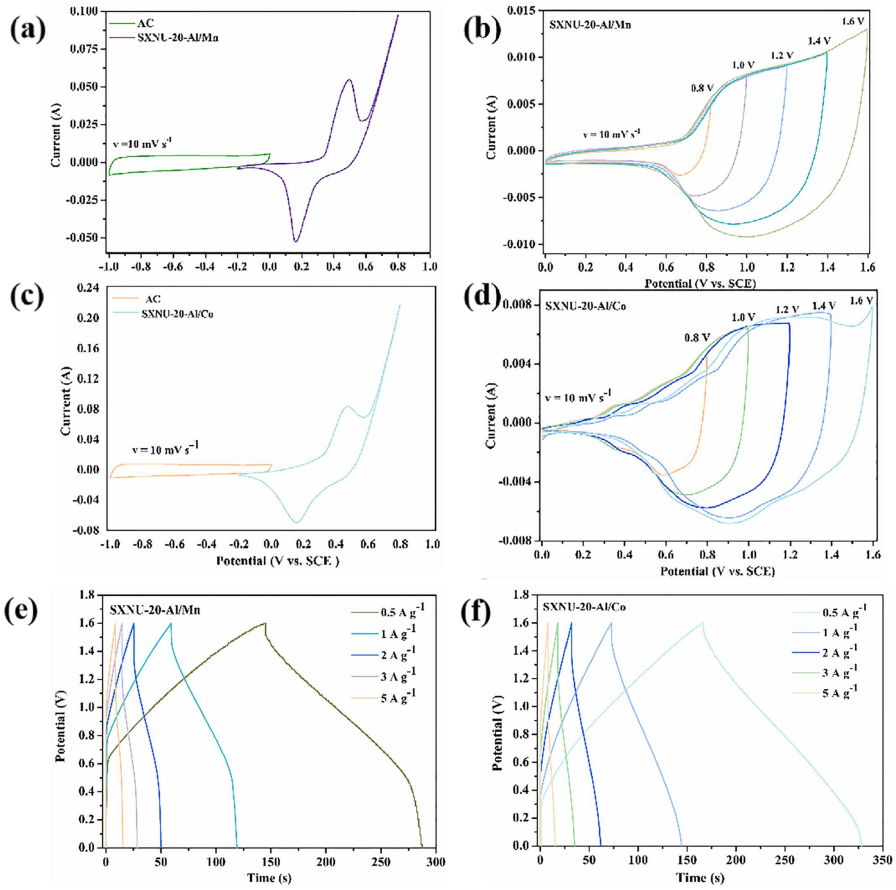

Fig. S8. An illustration of the asymmetric supercapacitor with the SXNU-20-Al/M (M = Mn, Co) positive electrode and AC negative electrode: (a) for SXNU-20-Al/Mn, (c) for SXNU-20-Al/Co; Cyclic voltammetry (CV) curves of (b) SXNU-20-Al/Mn and (d) SXNU-20-Al/Ni electrodes at a scan rate of 10 mV s^{-1}; Two-electrode capacitor performance: Galvanostatic charge-discharge curves of (e) SXNU-20-Al/Mn and (f) SXNU-20-Al/Co at different current densities.